Electronic Supplementary Material (ESI) for Nanoscale Advances.

Single-step assembly of gold nanoparticles into plasmonic colloidosomes at the interface of oleic acid nanodroplets

José Mª López-de-Luzuriaga,[a] Miguel Monge,*[a] Javier Quintana[a] and María Rodríguez-Castillo[a]

Electronic Supplementary Information

Table S1. Summary of the synthetic approaches, size of Au NPs and Au CSs, plasmon absorption and properties study for recently reported Au CSs.

Synthesis	**Size**	**Plasmon absorption**	**Properties**	**Ref**
SiO_2 nanosphere template	Au NPs: 13 nm Au CSs: 160-500 nm	NIR region	Encapsulation of large Au NPs. Colloidosome disruption with GSH	1
Oil-water emulsion	Au NPs: 12 nm Au CSs: > 1 μm	NIR region	Control of Au NP packing with ligands.	2
NH_2-SiO_2 dendritic templates	Au NPs: 3-10 nm Au CSs: hundreds of nm	Visible-NIR region. Tuning through cycle-by-cycle addition of Au NPs	Solar energy harvesting (nanoheaters) Raman thermometry Plasmonic catalysis	3
Oil-water emulsion with PVP	Au NPs: 3.7 nm Au CSs: < 100 nm	NIR region. Tuning with interparticle distance	SERS Catalytic activity of Au-Pd CSs	4
Reverse water-in-oil emulsion	Au NPs: 98 nm Au CSs: 0.5 – 5 μm	Broad absorption in the Vis-NIR	Plasmonic properties of black gold	5
Oleic acid nanodroplets in *n*-hexane	Au NPs: 3-5 nm Au CSs: < 200 nm	NIR region. Tuning with size, shape and interparticle distance	White-light induced photothermal properties OA-GSH ligand exchange Assembly-disassembly	This work

Table S2. Summary of experimental conditions and Au CSs morphology.

Au CSs	[Au(C_6F_5)(tht)] (mM)	Oleic acid (M)	Au:OA ratio	Au NP diameter (nm)	Au CSs diameter (nm)
1	8.8	0.128	1:14.5	4.0 ± 1.5	179 ± 29
2	4.4	0.128	1:29	3.1 ± 0.9	139 ± 23
3	13.2	0.128	1:9.7	4.2± 1.6	185 ± 23
4	8.8	0.064	1:7.3	3.3 ± 1.1	192 ± 32
5	8.8	0.380	1:43.2	2.9 ± 0.7	173 ± 27
6[a]	8.8	0.128	1:14.5	4.2 ± 1.4	189 ± 31

[a] Au CSs **6** is similar to Au CSs **1** but using a larger excess of TIPS

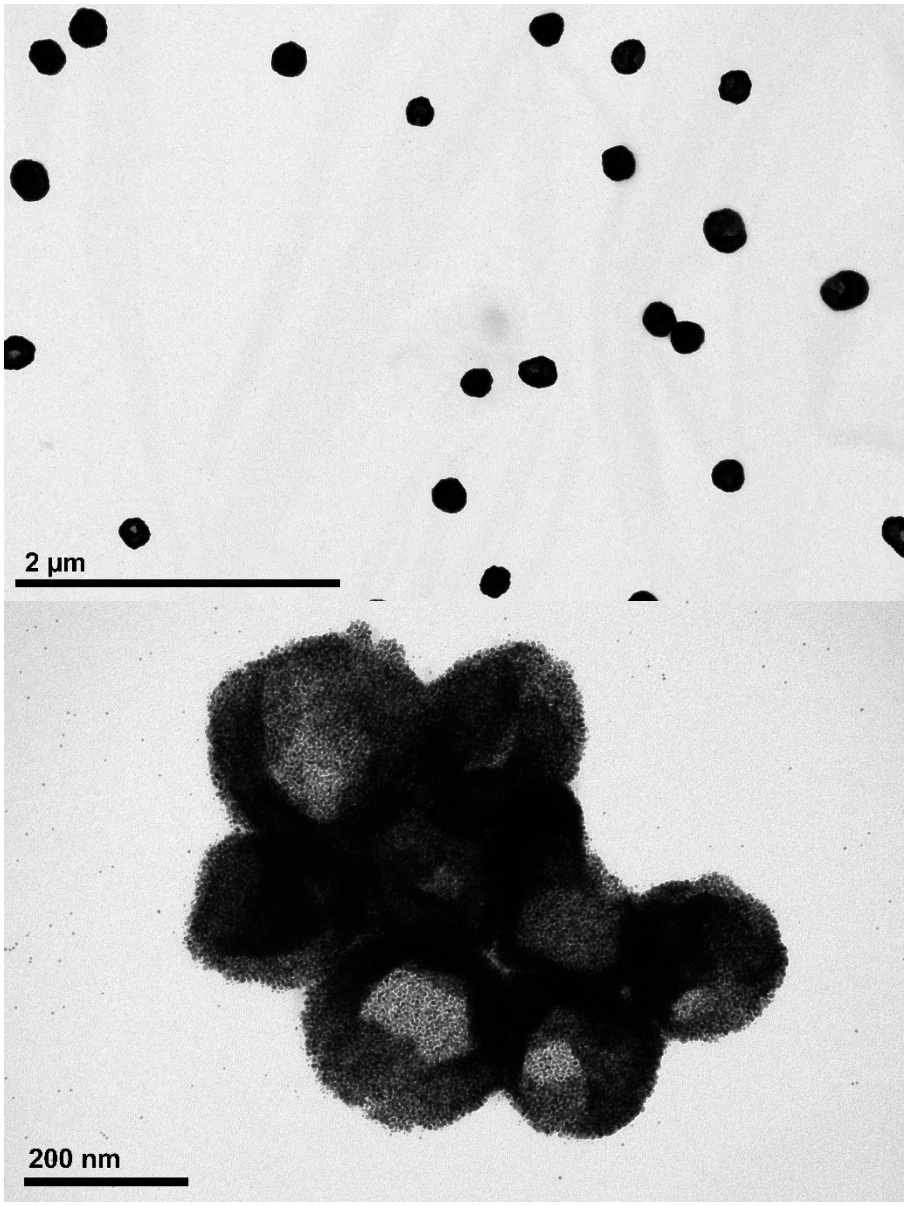

Fig. S1. TEM images of Au CSs (**6**)

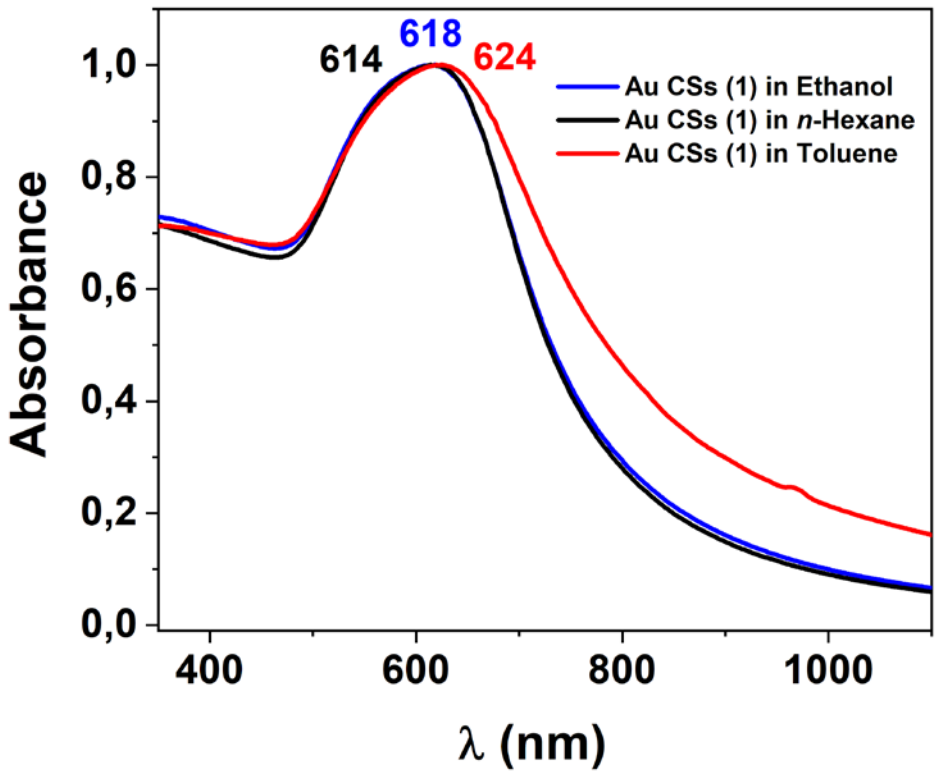

Fig. S2. UV/Vis/NIR spectrum of Au CSs (**1**) in different solvents.

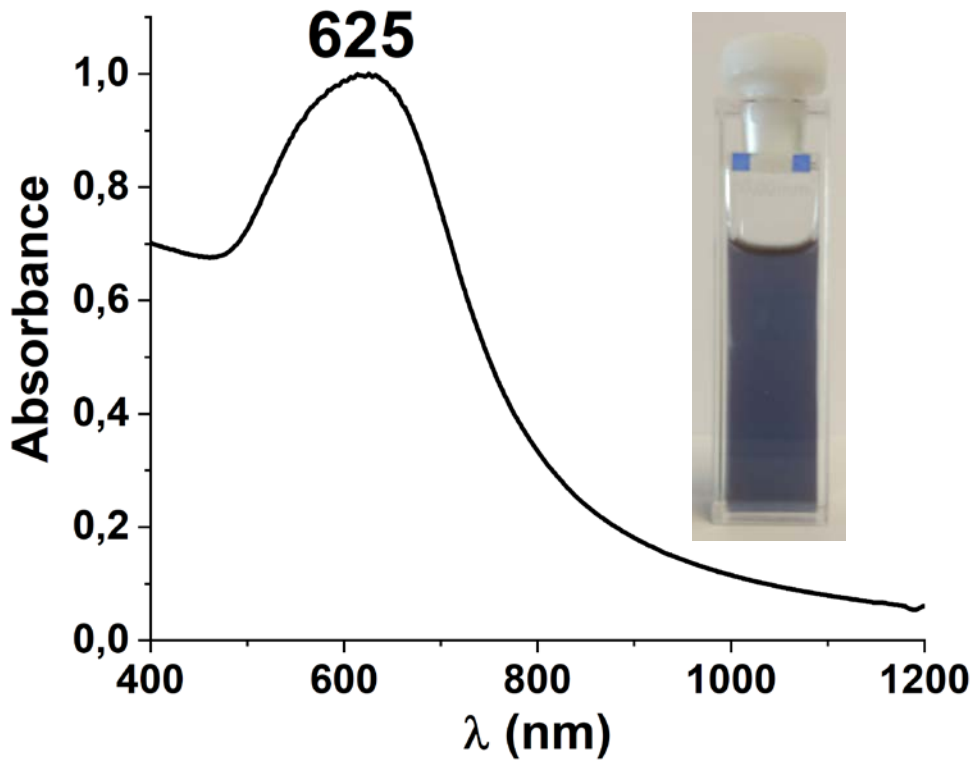

Fig. S3. UV/Vis/NIR spectrum of Au CSs (**6**) in *n*-hexane.

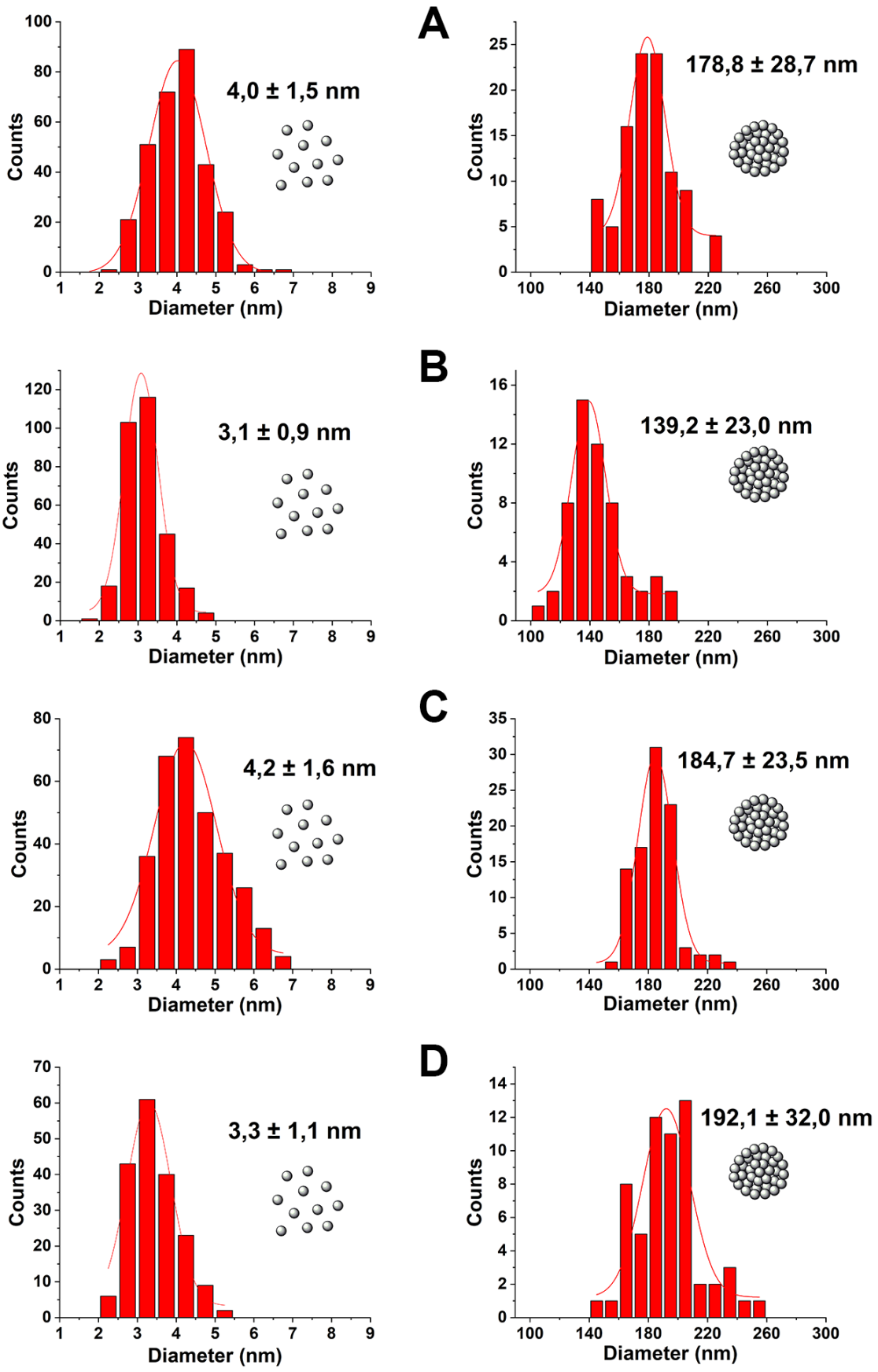
A
4,0 ± 1,5 nm
178,8 ± 28,7 nm
B
3,1 ± 0,9 nm
139,2 ± 23,0 nm
C
4,2 ± 1,6 nm
184,7 ± 23,5 nm
D
3,3 ± 1,1 nm
192,1 ± 32,0 nm
Counts
Diameter (nm)

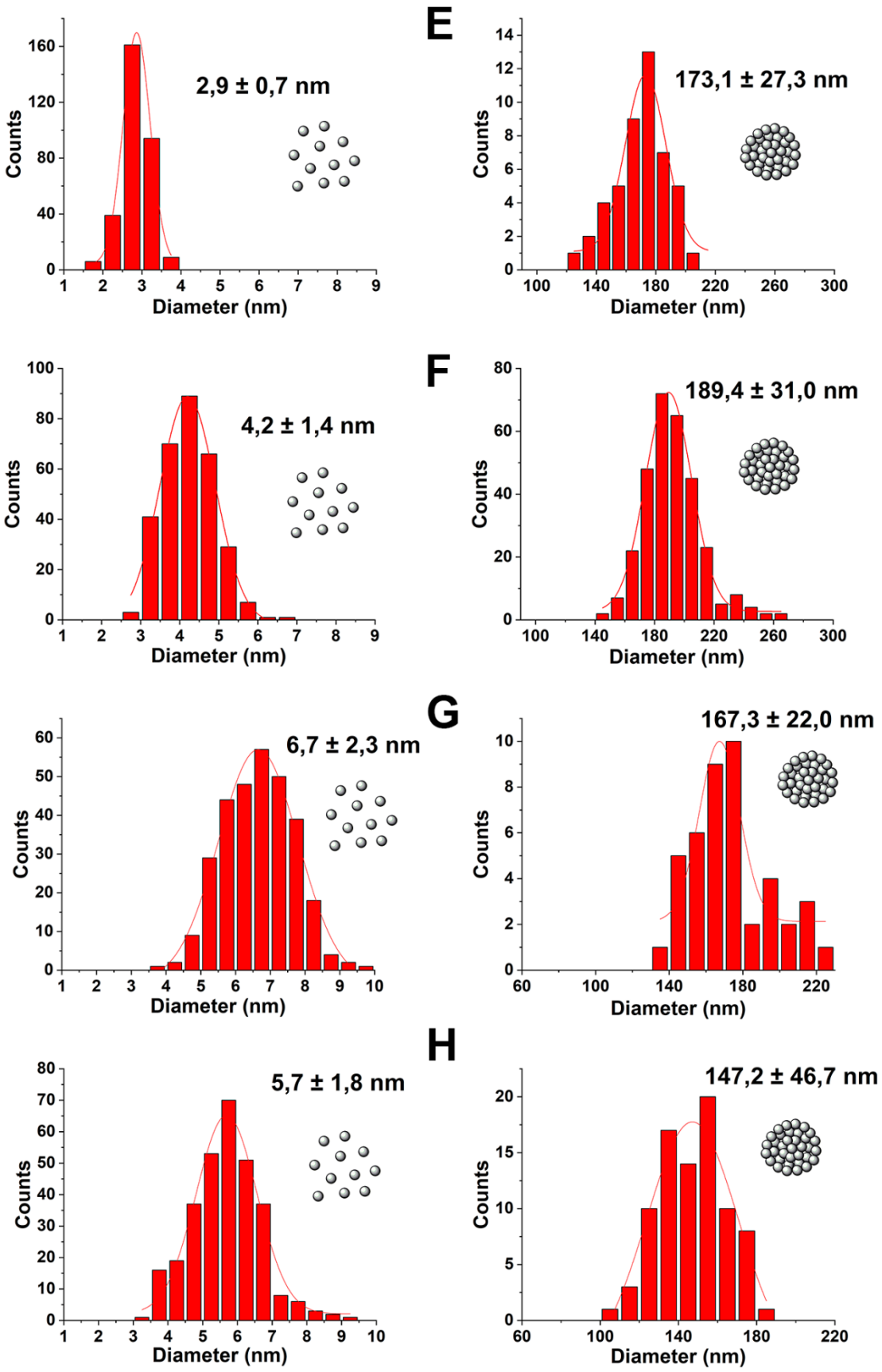
2,9 ± 0,7 nm
Counts
Diameter (nm)
E
173,1 ± 27,3 nm
Counts
Diameter (nm)
4,2 ± 1,4 nm
Counts
Diameter (nm)
F
189,4 ± 31,0 nm
Counts
Diameter (nm)
6,7 ± 2,3 nm
Counts
Diameter (nm)
G
167,3 ± 22,0 nm
Counts
Diameter (nm)
5,7 ± 1,8 nm
Counts
Diameter (nm)
H
147,2 ± 46,7 nm
Counts
Diameter (nm)

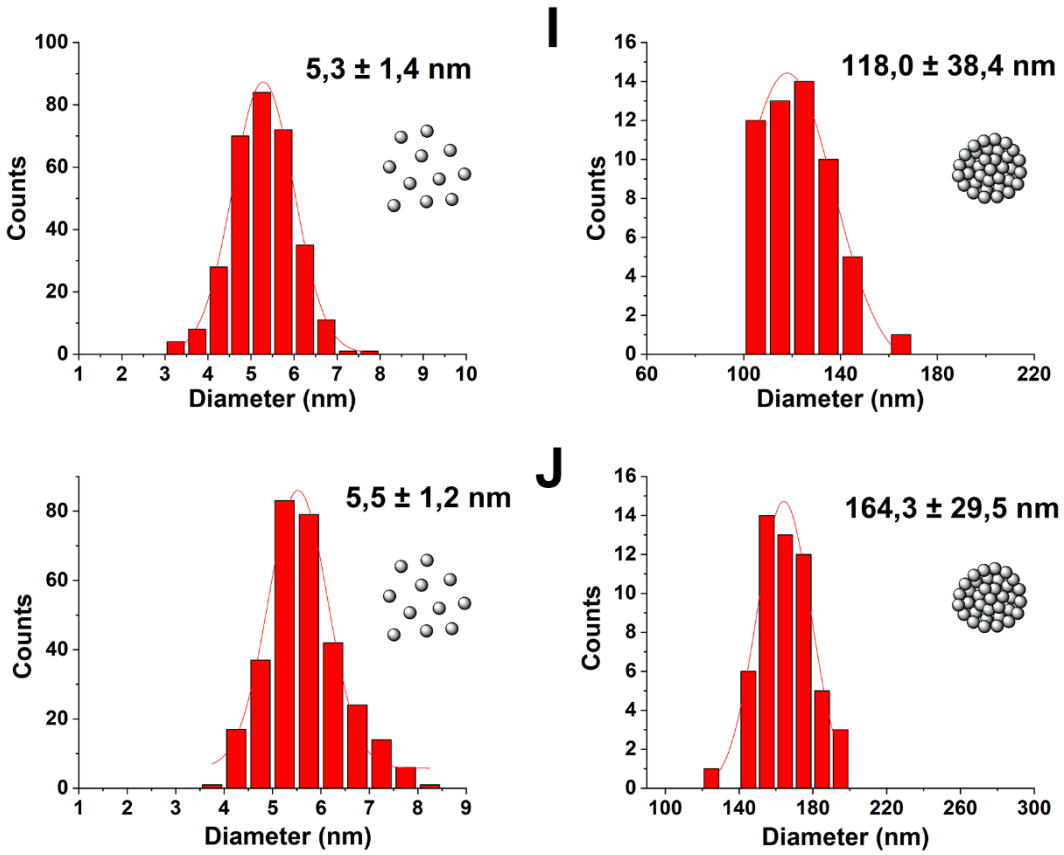

Fig. S4. Diameter distribution of Au CSs (right), and the spherical nanoparticles at their surface (left) for (**1** (A), **2** (B), **3** (C), **4** (D), **5** (E), **6** (F), **7** (G), **8** (H), **9**(I) and **10** (J)).

Spectroscopic studies

We have studied the ^{1}H, $^{13}C\{^{1}H\}$ and ^{19}F NMR spectra of samples of oleic acid (OA) and mixtures of OA and [Au(C_6F_5)(tht)] in 1:1 molar ratio, both in d8-THF and in d8-toluene. The latter solvent has been used as low-polar solvent, replacing *n*-hexane, since Au CSs are also formed in toluene in the same way as in *n*-hexane. From this study we can extract several interesting conclusions. Thus, the ^{1}H signal of the acidic proton of OA in d8-toluene appears shifted upfield and broadened when it is mixed with [Au(C_6F_5)(tht)] complex. In the same way, the $^{13}C\{^{1}H\}$ NMR spectrum also shows the signal attributed to the C atom of the carboxylic group shifted upfield. This could be interpreted in terms of an interaction between the –COOH carboxylic group of OA and the Au(I) complex. Since the tetrahydrothiophene ligand is labile towards its coordination to Au(I), the possibility of interaction of OA with the Au(I) centre through the C=O group, by the displacement of the tht ligand was also envisaged. This type of C=O coordination to Au(I) is not common but it has been previously reported for an NHC-Au-amide complex.[6] It is also important to note that the same comparison between the ^{1}H NMR spectra of OA and OA+[Au(C_6F_5)(tht)] complex using d8-THF as solvent does not give rise to the same result. Indeed, when d8-THF is used as solvent the ^{1}H signal of the acidic proton of OA appears broadened and at the same position in the presence and in the absence of the Au(I) complex, suggesting that in this polar solvent there is not any type of interaction between OA and the Au(I) complex (see Figures S5 and S6).

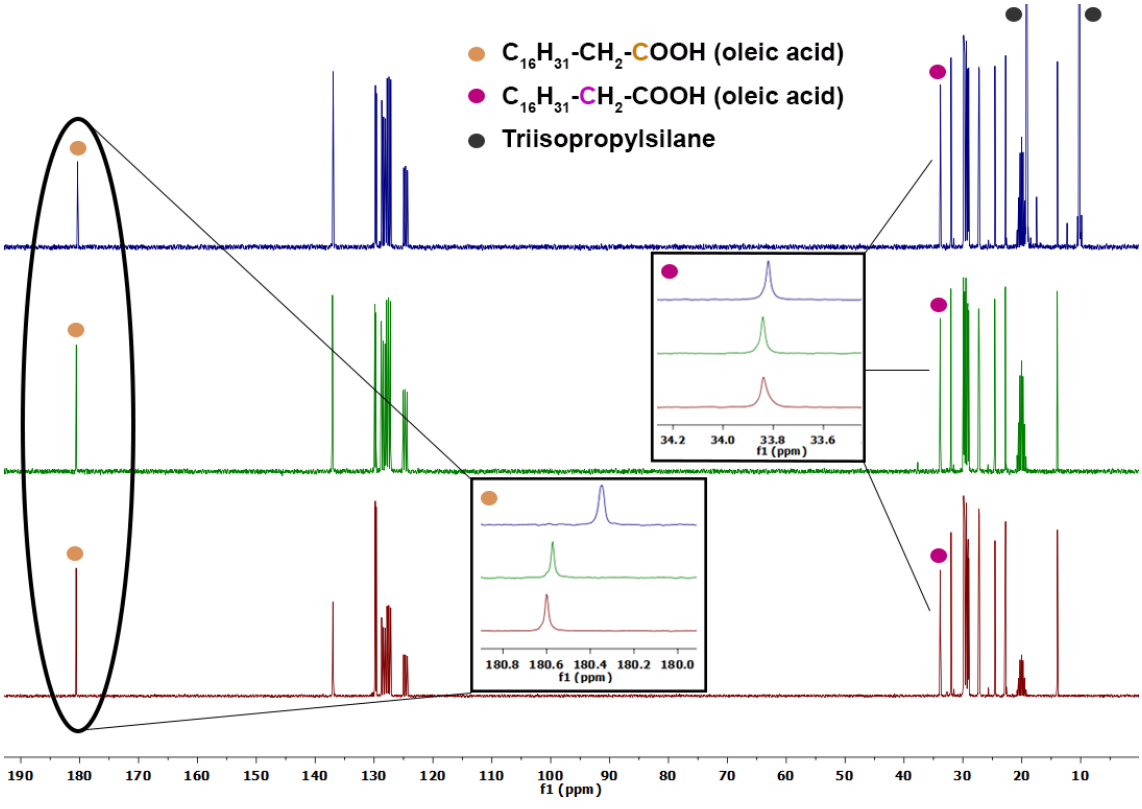

Fig. S5. $^{13}C\{^{1}H\}$ NMR spectra of OA in d8-Toluene (red); OA + TIPS (green) and OA + TIPS + [Au(C_6F_5)(tht)] (blue).

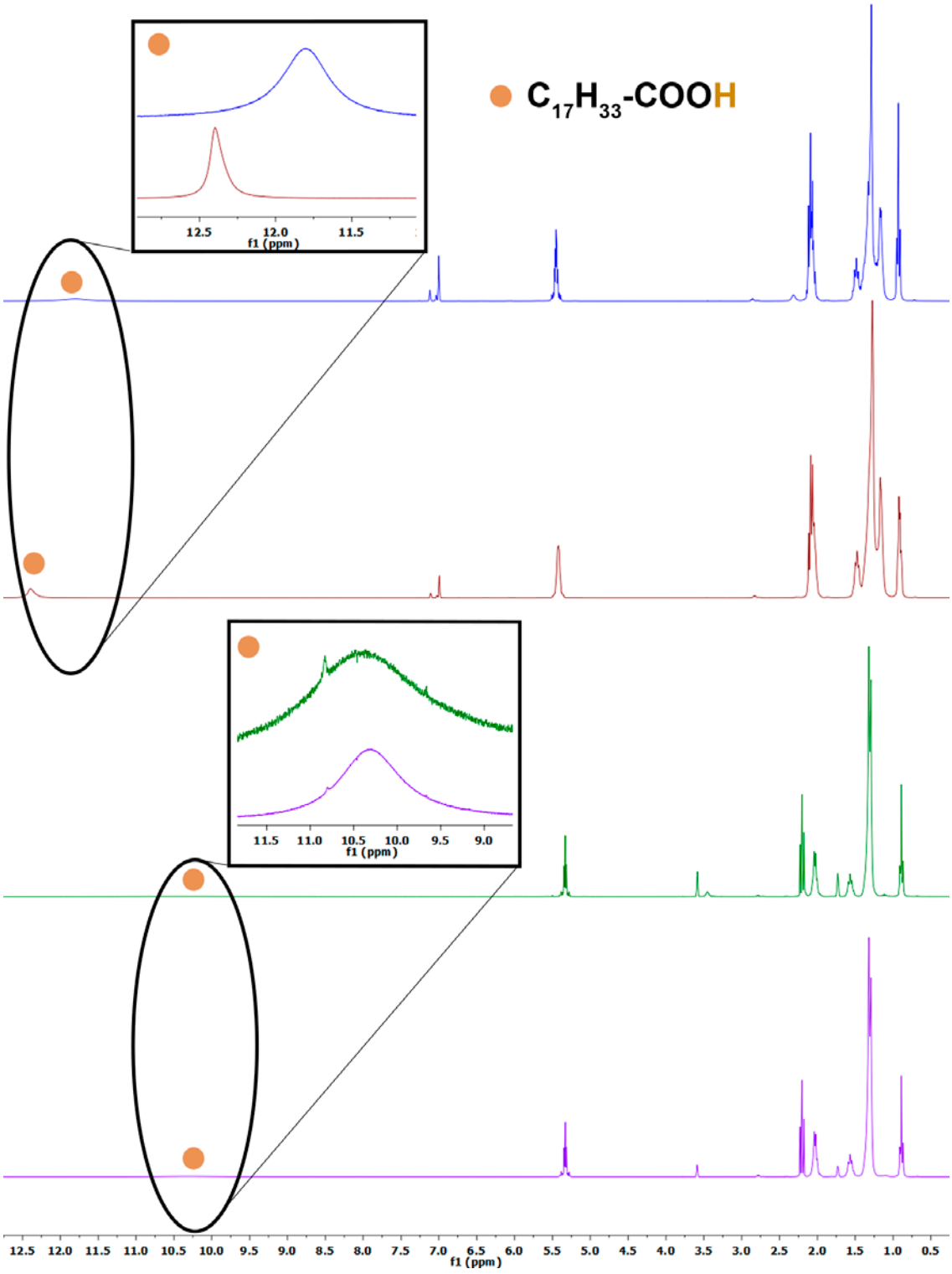

Fig.S6. ^{1}H NMR spectra of OA in d8-THF (purple) or d8-Toluene (red) and ^{1}H NMR spectra of the 1:1 mixture of OA and [Au(C_6F_5)(tht)] in d8-THF (green) or d8-Toluene (blue).

In addition, apart from the shift and broadening of the signal corresponding to the acidic proton of oleic acid in the ^{1}H spectrum, the MS-ESI spectra in negative mode shows the presence of the fragment $[Au(C_6F_5)(oleate)]^-$, what would support the formation of the proposed intermediate (see Figure S7).

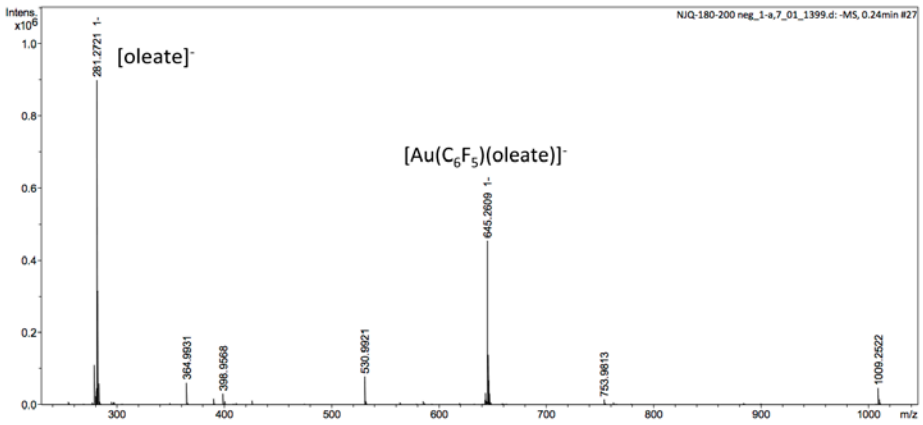

Fig. S7. ESI(-) MS spectrum of the 1:1 mixture of OA and $[Au(C_6F_5)(tht)]$

We have also used NMR techniques to observe the changes at molecular level during the formation of Au CSs (**1**) by using multinuclear magnetic resonance technique in solution. A preliminary observation was the ^{19}F NMR spectrum of a mixture of oleic acid and $[Au(C_6F_5)(tht)]$. In contrast to the spontaneous deprotonation of oleic acid with $C_6F_5^-$ ligands acting as base and formation of C_6F_5H previously observed for the bimetallic complex $[Au_2Ag_2(C_6F_5)_4(OEt_2)_2]_n$,[7] in the present case no reaction took place, probably due to the stronger biding of the perhalophenyl ligand to the Au(I) centre. Nevertheless, addition of the reducing agent TIPS triggers this process and the reduction of Au(I) takes place at the same time that C_6F_5H molecules are detected in the ^{19}F NMR spectrum in d8-toluene (where blue solutions of Au CSs are also formed like in *n*-hexane) as depicted in Figure S8 after 1 h of reaction. After 2h the entire complex is reduced forming the Au NPs that self-assemble into AuCSs. Washing of the Au CSs eliminates the presence of residual C_6F_5H or tht, leaving the oleic acid molecules as capping ligands for Au CSs.

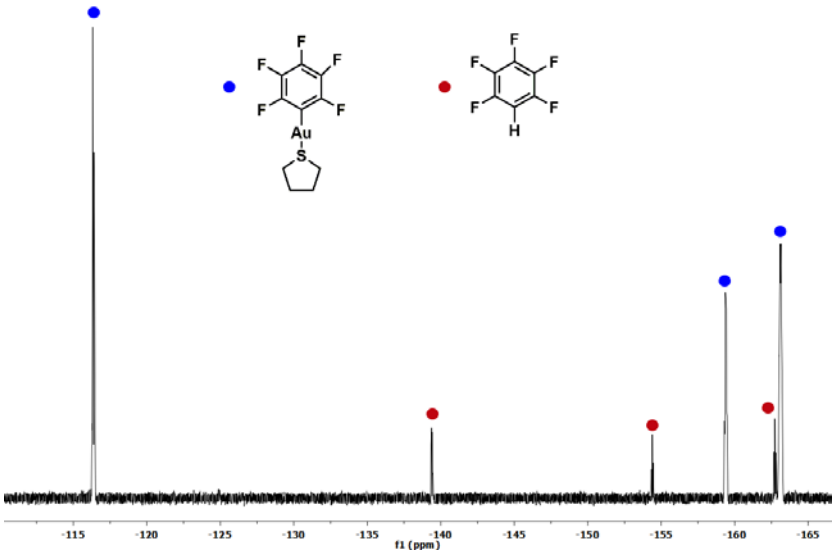

Fig. S8. ^{19}F NMR spectrum of Au CSs (**1**) preparation in d8-Toluene after 1h reaction. It can be observed the appearance of $[C_6F_5H]$ as a reaction by-product in the formation process.

We have studied the $^{13}C\{^{1}H\}$ and ^{1}H NMR spectra of washed Au CSs (**1**) in d8-Toluene. The results show a large upfield shift (1.5 ppm) of the signal assigned to the C atom of the carboxylic group and some upfield shift (0.3 ppm) of the signal of the a α C atom adjacent to the COOH group, but there is not any signal broadening or disappearance (see Figure S9). These results would agree with the interaction of the polar carboxylic group of oleic acid with the nanoparticle surface.

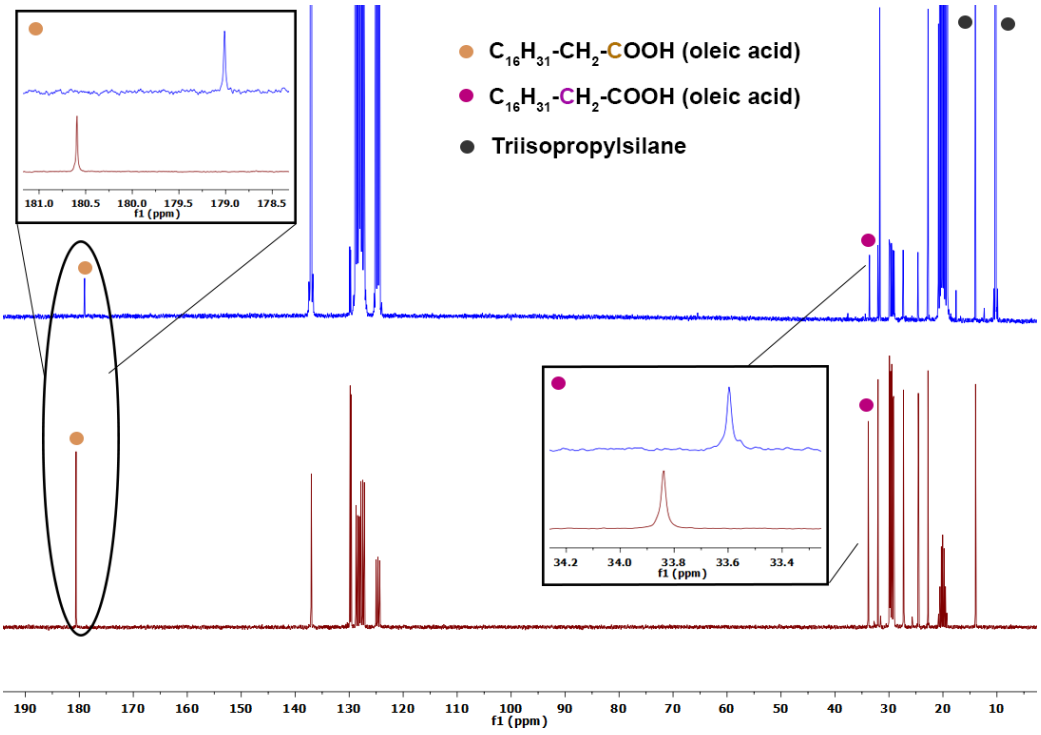

Fig. S9. $^{13}C\{^{1}H\}$ NMR spectra of OA (red) and washed Au CSs (**1**) (blue)

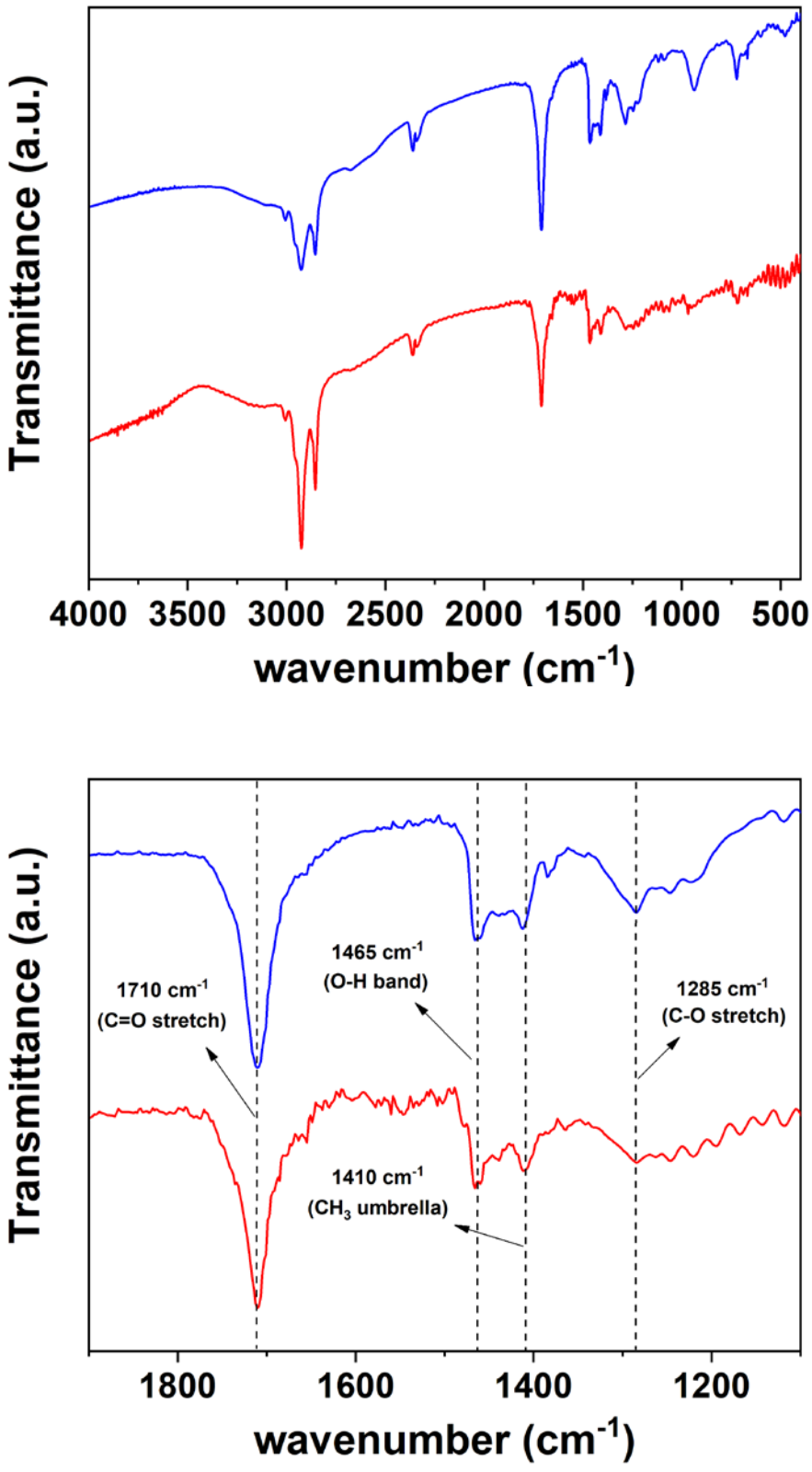

Fig. S10. IR spectra of OA (blue) and washed Au CSs (**1**) (red) on KBr disks (up). Detail of the 1200-1800 cm^{-1} region of the IR spectra.

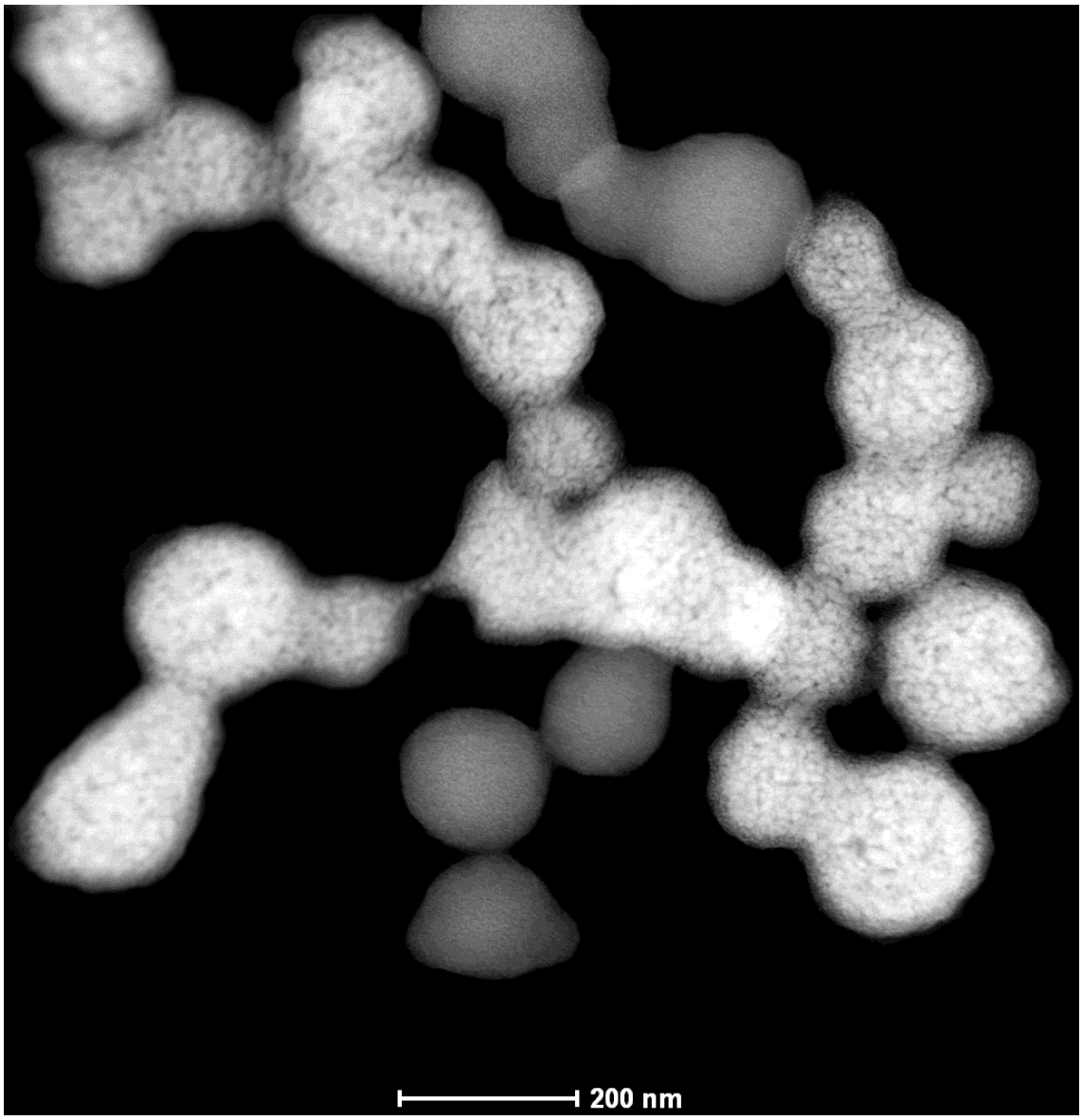

Fig. S11. HAADF-STEM image of the nanostructures formed after the disassembly/reassembly of Au CSs (**1**).

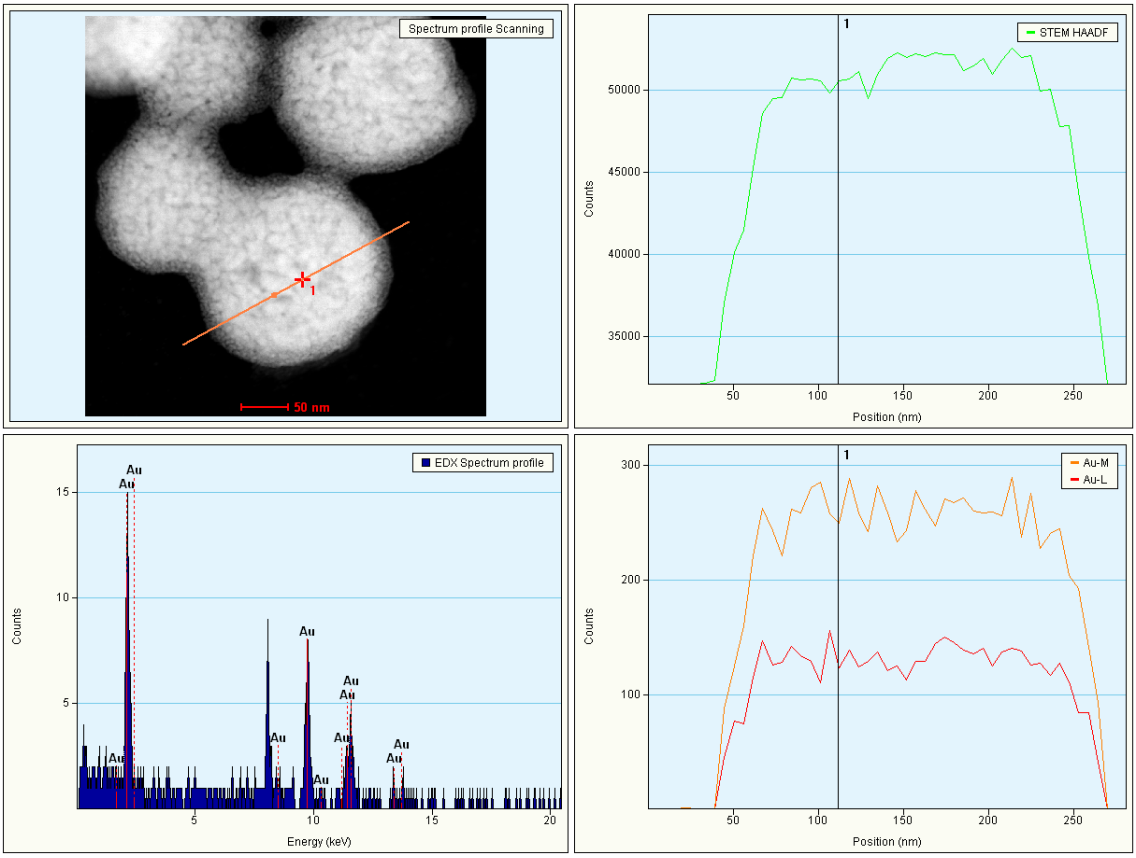

Fig. S12. HAADF-STEM image (up-left): HAADF line scan intensity profile (up-right); energy-dispersive X-ray (EDX) spectra (bottom-left) and line-scan elemental gold profiles (bottom-right) for the nanostructures formed after the disassembly/reassembly of Au CSs (**1**).

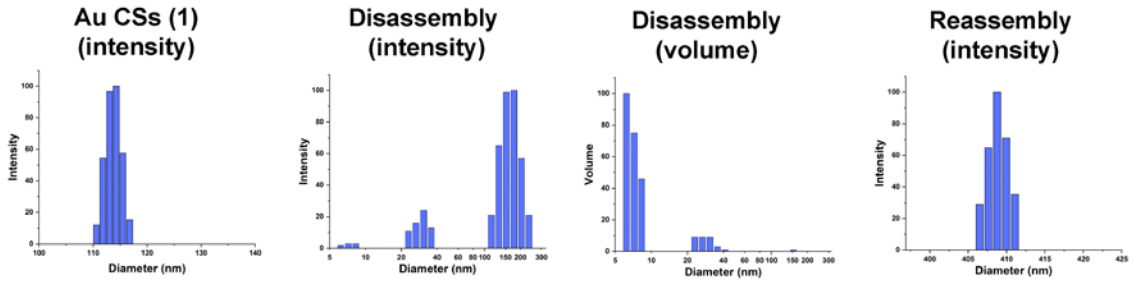

Fig. S13. DLS measurements of the nanostructures involved in the disassembly/reassembly of Au CSs (**1**).

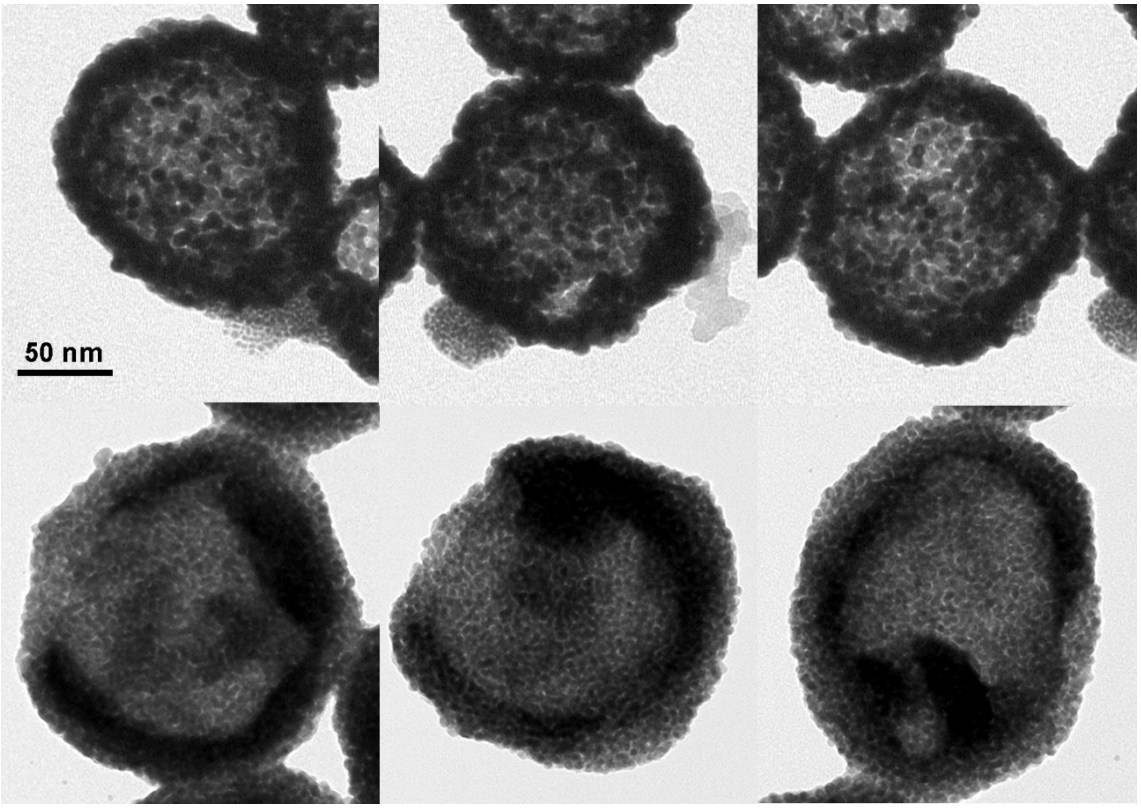

Fig. S14. TEM images of Au CSs (**10**) (top) and Au CSs (**6**) (bottom), both in ethanol solutions. With these images it can be shown that the surface of Au CSs (**6**) appear less compact, what could be related to the ease of opening of these CSs upon GSH addition.

References

1 M. Liu, Q. Tian, Y. Li, B. You, A. Xu and Z. Deng, *Langmuir*, 2015, **31**, 4589–4592.

2 K. Larson-Smith and D. C. Pozzo, *Langmuir*, 2012, **28**, 11725–11732.

3 M. Dhiman, A. Maity, A. Das, R. Belgamwar, B. Chalke, Y. Lee, K. Sim, J. M. Nam and V. Polshettiwar, *Chem. Sci.*, 2019, **10**, 6594–6603.

4 L. Zhang, Q. Fan, X. Sha, P. Zhong, J. Zhang, Y. Yin and C. Gao, *Chem. Sci.*, 2017, **8**, 6103–6110.

5 D. Liu, F. Zhou, C. Li, T. Zhang, H. Zhang, W. Cai and Y. Li, *Angew. Chem. Int. Ed.*, 2015, **127**, 9732–9736.

6 R. S. Ramón, S. Gaillard, A. Poater, L. Cavallo, A. M. Z. Slawin and S. P. Nolan, *Chem.–Eur. J.*, 2011, **17**, 1238-1246.

7 J. Crespo, J. M. López-de-Luzuriaga, M. Monge, M. Elena Olmos, M. Rodríguez-Castillo, B. Cormary, K. Soulantica, M. Sestu and A. Falqui, *Chem. Commun.*, 2015, **51**, 16691–16694.